ELSEVIER

Polymer 44 (2003) 223–237

polymer

www.elsevier.com/locate/polymer

Particle formation under monomer-starved conditions in the semibatch emulsion polymerisation of styrene. Part II. Mathematical modelling

Shahriar Sajjadi*

Division of Engineering, King's College London, London, WC2R 2LS UK

Accepted 30 September 2002

Abstract

Models, together with a comparison with experimental data, are presented for the particle nucleation under monomer-starved conditions. In the first model, simplifications were made to obtain analytical solutions. The Smith and Ewart theory was extended to include particle formation under monomer-starved conditions. It was assumed that the rate of particle growth is controlled by the rate of monomer addition. An appropriate correlation for prediction of number of polymer particles in terms of surfactant and initiator concentrations and monomer addition rate was derived as $N_p = k(a_s[S])^{1.0} R_I^{2/3} R_a^{-2/3}$. The second model takes advantage of the new developments in understanding of the kinetics of the water phase and its effects on the radical capture efficiency of micelles. The model accounts for monomer solubilisation in the micelles. According to the model predictions, the size of micelles and their aggregation number are subject to variation during nucleation. The model could successfully predict some important features of particle formation under monomer-starved conditions.

Keywords: Particle nucleation; Semibatch emulsion polymerisation; Micelles

1. Introduction

Smith and Ewart (SE) developed a theory for particle formation that applies to monomers such as styrene [1]. According to the SE theory, the number of polymer particles, N_p, generated in a conventional batch process is shown by the following expression:

$$N_p = k\left(\frac{R_I}{\mu}\right)^{2/5} (a_s[S])^{3/5} \quad (1)$$

where k is a numerical constant, μ the volumetric growth rate per particle in interval I, R_I the rate of radical generation in the water phase, a_s the adsorption area occupied by a molecule of emulsifier on the surface of polymer particles and $[S]$ the concentration of emulsifier per unit volume of water. It is clear from Eq. (1) that N_p is inversely proportional to $\mu^{2/5}$. μ is given by Ref. [2]

$$\mu = \frac{k_p \rho_m \varphi_m}{N_A \rho_p \varphi_p} \quad (2)$$

where k_p is propagation rate constant, ρ_m and ρ_p are densities of monomer and polymer, respectively, and φ_m and φ_p are volume fractions of monomer and polymer in the polymer particles at saturation conditions, respectively. In a conventional batch emulsion polymerisation, the rate of particle growth is thermodynamically controlled at a constant level by monomer diffusion from the monomer droplets to the polymer particles. In semibatch processes, the rate of particle growth can be controlled by the rate of monomer addition. Monomer-starved semibatch emulsion polymerisation with the neat monomer feed is a process in which monomer is continuously added to the reactor containing an aqueous solution of emulsifier and initiator. The major requirements for maintaining the starved conditions are that 1) polymerisation starts with no or a little monomer in the initial reactor charge and 2) the rate of monomer addition is kept at a low level. Particle nucleation under monomer-starved conditions can result in generation of a larger number of polymer particles, compared to conventional batch processes [3–6]. While the reason for this has been conceptually explained [3–6], to date no theoretical predictions for the number of particles have been reported in the literature. This seems to be odd because the predictions of number of particles generated in continuous

* Tel.: +44-20-7848-2682; fax: +44-20-7848-2932.
E-mail address: shahriar.sajjadi-emami@kcl.ac.uk (S. Sajjadi).

0032-3861/03/$ - see front matter © 2002 Elsevier Science Ltd. All rights reserved.
PII: S0032-3861(02)00735-8

Nomenclature

a	partition coefficient of monomer ($[M]_p/[M]_w$)
a_s	area of polymer particle covered by one molecule of emulsifier
$a_{t,\tau}$	surface area of particles formed at τ at the time t
A_p	total area of polymer particles
D_i	diffusion coefficient of a radical with chain length i in the water phase
D_p, D_w	diffusion coefficients of monomer radicals in the polymer particles and water phase, respectively
$[E^\circ]$	concentration of monomeric radicals formed by transfer to monomer in the water phase
f	efficiency factor for the initiator
j_{crit}	critical length for radical precipitation
$[I]$	initiator concentration
$[IM_i]$	water phase concentration of i-meric radicals
k_d	rate coefficient for initiator decomposition
k_{dM}	rate coefficient for desorption of a monomer radical from a polymer particle
k_{am}^i	rate coefficient for entry of i-meric radical formed by initiator decomposition into a micelle
k_{ap}^i	rate coefficient for entry of i-meric radical formed by initiator decomposition into a polymer particle
k_{eE}	rate coefficient for re-entry of desorbed radicals into a polymer particle
k_p^1	propagation rate constant of monomeric radical formed by transfer to monomer
k_p, k_{p0}	overall propagation rate constant in polymer phase
k_{pw}^i	water phase propagation rate constant for i-meric radicals
k_{pw}	water phase propagation rate constant
k_{tr}	rate constant for transfer to monomer
k_{tw}	water phase termination rate constant
$[M]$	total number of moles of monomer in the reacting latex per litre of the water phase
$[M]_0$	initial monomer concentration in the reactor
$[M]_m$	the number of moles of monomer solubilised in micelles per litre of water phase
M_{mon}	molecular weight of monomer
$[M]_p$	monomer concentration within polymer particles
$[M]_{p,sat}^{\infty}$	saturation concentration of monomer within the large polymer particles
$[M]_{p,sat}$	saturation concentration of monomer within the polymer particles
$[M]_t$	total number of moles of monomer in the recipe per litre of the water phase
$[M]_w$	monomer concentration in the water phase
$[M]_{w,sat}$	monomer concentration in the water phase in the presence of monomer droplets
n_{agg0}, n_{agg}	micellar average aggregation number in monomer-free water phase and water phase at the polymerisation conditions, respectively
$\bar{n}$	average number of radicals per particle
N_A	Avogadro's number
N_p	total number of particles in the reactor per litre of water phase
N_0	number of particles that contain no radical per litre of water phase
N_1^m	number of particles that contain one monomeric radical per litre of water phase
N_1^p	number of particles that contain one polymeric radical per litre of water phase
N_m	concentration of micelles in the water phase
$[P]$	number of moles of monomer converted to polymer per litre of water phase
r_m	radius of micelles
r_p	average radius of monomer-swollen polymer particles
R_a	rate of monomer addition
R_I	rate of initiator decomposition
R_p	rate of polymerisation
$[R^\circ]$	total concentration of radicals in the water phase
S_{CMC}	critical micellar concentration
$[S]$	emulsifier concentration
t, τ	time
T	temperature

stirred tank emulsion polymerisation reactors with SE theory were also reported in the literature long ago [7–10].

The theory for particle formation has appreciably advanced in the last decades. Following the genuine development of SE, many aspects of particle formation were reinvestigated by different research groups and new schemes for radical entry and radical desorption have been introduced to particle formation by taking into account the kinetics of chemical reactions and physical transport of moieties occurring in the water phase [11–14]. More detailed insights into particle formation have been given in the last chapter of the excellent book by Gilbert [15]. Simultaneously, the SE based treatments of the nucleation phenomena, with incorporation of radical desorption, are being widely used for simplicity in scope and the ability to predict the trend of particle formation which is of interest to both industry and academia.

The objective of this research work was to explain and predict the dependence of particle number and also the evolution of monomer conversion on emulsifier concentration, initiator concentration, and monomer feed rate in the monomer-starved semibatch emulsion polymerisation of styrene.

2. Models description

Two different levels of modelling are considered. In the first approach, we are concerned with a polymerisation system for which it is assumed that the basic equations describing its behaviour is known theoretically but for which no analytical solution exist, and consequently a numerical solution will be sought instead. It is often necessary to define a mathematical model, which will reduce the complexity of the original basic equations and make it tractable within fixed limits. This, of course, might result in a less accuracy of the model predictions, however, because of its simplicity, it can better explain the physical concept of the modelling and the underlining theory. For this reason, we first present a simple model, which is hereafter called model I, to address particle nucleation under monomer-starved conditions. In model II, a more rigorous approach is considered for prediction of both particle formation and rate of polymerisation.

2.1. Model I

The SE case-II theory is extended to cover particle formation under monomer-starved conditions. The fundamental assumptions of the SE theory are

1. Particle formation occurs by micellar mechanism. The free radicals generated by initiator in the water phase are absorbed in emulsifier micelles. The rate of absorption is either assumed constant or decreasing with time because of competition with new particles.
2. The rate of radical entry into micelles or polymer particles is proportional to their surface area.
3. Nucleation stops when all surfactant molecules have been consumed by adsorption onto the new particles.

First assumption ignores the radical loss due to termination in the water phase. Assumptions 2 and 3 are still widely used for modelling of emulsion polymerisation systems [16,17]. The SE case-II theory for particle formation suffers an important drawback, that is, it ignores radical desorption from polymer particles. The radical desorption in emulsion polymerisations can increase the number of polymer particles in two different ways: (a) by decreasing the growth period of the active particles and (b) by entry of desorbed radicals into micelles converting them into particles. For styrene emulsion polymerisation the desorbed radicals do not directly contribute to the particle formation by entering micelles, because their fate is to re-enter the particles [18,19]. Thus, exit might only increase the number of particles through reducing the rate of growth of particles (it should be noted that some of the desorbed radicals terminate in the water phase with the initiator-derived radicals, which otherwise could enter micelles. This might even lead to a decrease in N_p under some circumstances). In the SE theory, the volumetric growth rate of a particle is assumed to be constant in the interval of particle formation. The constant volume growth rate of particles, defined in Eq. (2), is based on this assumption that all particles during nucleation contain one radical. In the model developed here the first three assumptions of the SE theory are retained and the following new assumption is made.

4. The rate of growth of particles is not constant and is controlled by the rate of monomer addition. This requires that monomer transfer from the fed-in monomer droplets to the polymer particles be instantaneous so that no monomer droplets are formed in the reaction mixture during feeding.

The above assumption indicates that the effects of all events that might contribute to the reduction in the rate of growth of particles, such as radical desorption from particles or radical termination in the particles, have been indirectly taken into consideration. In this model, the kinetics of water phase is ignored, a restriction that will be lifted with the second model.

The volumetric growth rate of a particle is defined by

$$\mu(t) = \frac{dv_p}{dt} \tag{3}$$

where v_p is the volume of the polymer particle. The volumetric growth rate of a particle in a monomer-starved semibatch process is given by the following

expression [5]

$$\mu(t) = \frac{\left[1 - w_p\left(1 - \frac{\rho_m}{\rho_p}\right)\right]R_a}{N_p} \quad w_p > w_{pcr} \tag{4}$$

where R_a is the rate of monomer addition in l/s l(aq), w_p is the polymer weight ratio in polymer particles, and w_{pcr} is the w_p at which interval III starts. In the above equation, the monomer solubilised in the micelles and dissolved in the water phase have been ignored. It is also assumed that the growth of particles is independent of their size. If the difference between monomer and polymer densities is neglected for simplicity, the volumetric growth rate of polymer particles can be shown by:

$$\mu(t) = \frac{R_a}{N_p} \tag{5}$$

Eq. (5) predicts a linear relation between the instantaneous rate of particle growth and the rate of monomer addition. It is apparent from Eq. (5) that for monomer-starved conditions, polymer particles compete for the monomer from the feed. As a result of continuous nucleation and increase in N_p, μ is a decreasing function of time during nucleation. Using Eqs. (3) and (5), the volume at time t of a particle formed at time τ is obtained as

$$v_{\tau,t} = R_a \int_\tau^t \frac{d\tau}{N_p} \tag{6}$$

Thus, the surface area at time t of a particle formed at time τ is

$$a_{\tau,t} = (36\pi)^{1/3} R_a^{2/3} \left(\int_\tau^t \frac{d\tau}{N_p}\right)^{2/3} \tag{7}$$

In order to solve the above equation, the variation of N_p with time should be known. According to the SE theory, the rate of particle formation, dN_p/dt, can be treated in two different ways.

Higher limit. This is an ideal case that the very small micelles capture all the free radicals being generated in the water phase as long as micelles are still present. This implies that the rate of particle formation is equivalent to the rate of formation of free radicals in the water phase: $R_I = 2fk_d[I]$. We assume that R_I is constant during nucleation, so,

$$\frac{dN_p}{dt} = R_I \quad \Rightarrow \quad N_p = R_I t \tag{8}$$

Thus, the area at time t of a particle formed at time τ is

$$a_{\tau,t} = (36\pi)^{1/3} \left(\frac{R_a}{R_I}\right)^{2/3} Ln^{2/3}(t/\tau) \tag{9}$$

The total area, A_p, of all particles present at time t is given by the integration

$$A_p = \int_0^t a_{\tau,t} \frac{dN_p}{d\tau} d\tau \tag{10}$$

Thus, using Eqs. (8) and (9) in the above equation, we have

$$A_p = (36\pi)^{1/3} \left(\frac{R_a}{R_I}\right)^{2/3} \int_0^t Ln^{2/3}(t/\tau) \frac{dN_p}{d\tau} d\tau \tag{11}$$

After integration

$$A_p = (36\pi)^{1/3} \Gamma(5/3) R_I^{1/3} R_a^{2/3} t \tag{12}$$

At time $t = t_f$, when the micelles disappear and particle nucleation ceases, $A_p = a_s[S]$, thus

$$t_f = 0.229(a_s[S]) R_I^{-1/3} R_a^{-2/3} \tag{13}$$

According to Eq. (13), the limited growth rate of particles prolongs the nucleation period and thus results in the formation of a large number of particles.

Since $N_p = R_I t_f$, the following equation is obtained for the final number of polymer particles

$$N_p = 0.23(a_s[S]) R_I^{2/3} R_a^{-2/3} \tag{14}$$

Lower limit. According to the SE theory, the other idealised situation is that in which polymer particles can compete with micelles for capturing radicals from the water phase. The efficiency of a given interfacial area for capturing radicals is assumed to be constant and to be independent of the size of particles or micelles on which it is situated.

The rate of particle formation is

$$\frac{dN_p}{dt} = R_I\left(1 - \frac{A_p}{a_s[S]}\right) \tag{15}$$

Using Eqs. (7) and (10), we have

$$A_p = (36\pi)^{1/3} R_a^{2/3} \int_0^t \left(\int_\tau^t \frac{d\tau}{N_p}\right)^{2/3} \frac{dN_p}{d\tau} d\tau \tag{16}$$

Insertion of the above equation into Eq. (15) will result in a complicated integro-differential equation, which cannot be easily solved analytically. Here, we assume that the surface area of particles formed at time τ at time t can be approximated by Eq. (9) derived for the higher limit. Thus, using Eq. (11) for A_p, Eq. (15) may be written as

$$\frac{dN_p}{dt} = R_I - (36\pi)^{1/3} (a_s[S])^{-1} R_I^{1/3} R_a^{2/3} \int_0^t Ln^{2/3}(t/\tau) \times \left(\frac{dN_p}{d\tau}\right) d\tau \tag{17}$$

The above equation can be solved by using Volterra's equation of the second type, which may be written as

$$\phi(x) = f(x) + \lambda \int_0^x K(x,z)\phi(z) dz \tag{18}$$

The solution of the above equation is given by the infinite series

$$\phi(x) = \sum_{n=0}^{\infty} \lambda^n \phi_n(x) \tag{19}$$

where

$$\phi_0(x) = f(x) \tag{20}$$

$$\phi_n(x) = \int_0^x K(x,z)\phi_{n-1}(z)\mathrm{d}z \tag{21}$$

Applying Eqs. (18)–(21) to Eq. (17), the desired solution may be expressed by the infinite series

$$\frac{\mathrm{d}N_\mathrm{p}}{\mathrm{d}t} = \rho \sum_{n=0}^{\infty} \frac{y^n}{(n!)^{5/3}} \tag{22}$$

where

$$y = -\frac{(36\pi)^{1/3}\Gamma(5/3)R_\mathrm{I}^{1/3}R_\mathrm{a}^{2/3}}{a_\mathrm{s}[S]}t = -\xi t \tag{23}$$

By using a method of successive approximation, the value of y which gives $\mathrm{d}N_\mathrm{p}/\mathrm{d}t = 0$ in Eq. (22), y_f, is found to be

$$y_\mathrm{f} = -\xi t_\mathrm{f} = -1.697 \tag{24}$$

Thus, the time t_f at which nucleation ceases is

$$t_\mathrm{f} = 0.389(a_\mathrm{s}[S])R_\mathrm{I}^{-1/3}R_\mathrm{a}^{-2/3} \tag{25}$$

The first few terms of Eq. (22) may be written out as

$$\frac{\mathrm{d}N_\mathrm{p}}{\mathrm{d}t} = R_\mathrm{I}\left(1 - \xi t + \frac{\xi^2 t^2}{(2!)^{5/3}} - \frac{\xi^3 t^3}{(3!)^{5/3}} + \frac{\xi^4 t^4}{(4!)^{5/3}} - \cdots\right) \tag{26}$$

The above equation can be integrated from $t = 0$ to $t = t_\mathrm{f}$, to give the final number of polymer particles produced. Integrating Eq. (26) and then substituting y_f and t_f from Eqs. (24) and (25), and after some manipulation, the total number of particles is obtained as:

$$N_\mathrm{p} = 0.16(a_\mathrm{s}[S])R_\mathrm{I}^{2/3}R_\mathrm{a}^{-2/3} \tag{27}$$

If Eqs. (15) and (16) are numerically solved, the constant obtained for the above equation is 0.13, while the exponents remain unchanged. This means that the assumption used in deriving the above equation will introduce 20% error in the constant with no effect on the exponents. Eq. (27) is identical with that obtained for the higher limit, except for the value of numerical constant. For the monomer-starved systems the actual constant should lie between those represented by Eqs. (14) and (27):

$$N_\mathrm{p} = k(a_\mathrm{s}[S])R_\mathrm{I}^{2/3}R_\mathrm{a}^{-2/3} \tag{28}$$

where $0.13\ (0.16) < k < 0.23$.

The above equation shows that for semibatch emulsion polymerisations under monomer-starved conditions, the number of particles is more sensitive to formulation variables than that for the monomer-flooded conditions. This is obvious by the higher power exponents of N_p for semibatch processes, compared with those for batch processes.

It is apparent from the results that as discussed later, while the experimental data approximate the SE prediction of exponents for N_p in terms of R_a, $[S]$, and $[I]$, the actual numerical values are significantly in error. This is because only a small fraction of radicals, f, contribute into particle formation. In the classical theory of SE, f is defined as efficiency of initiator decomposition and is constant. In fact, f is a function of initiator type, concentration and decomposition rate, number and size of latex particles and micelles, monomer concentration in the water phase, and the rate of radical termination in the water phase [14]. Here for simplicity, we use f as an adjustable parameter to the general scheme of the SE model.

2.2. Model II: a dynamic model

In a previous publication [4], we described the kinetics of the styrene emulsion polymerisation under monomer-starved condition. The model developed here is based on the characteristics found for that system. The model resembles those presented in the literature for the nucleation stage in batch emulsion polymerisations [13,15,17]. However, the model contains new features. The most important one is that it accounts for the partitioning of monomer among the polymer phase, water phase and micelles. The major assumptions are as follows:

- Micellar nucleation and homogeneous nucleation are considered. Although, the former is the main mechanism for particle formation under the conditions of this study.
- A full account of compartmentalisation is taken into consideration by assuming a zero–one system for the nucleation stage. In a zero–one system, the entry of a radical into a latex particle which already contains a growing radical results in instantaneous termination. Such an assumption can be extended to monomer-starved conditions because the radical entry into monomer-starved polymer particles is kinetically unimportant in view of the presence of large number of micelles competing for radicals.
- For simplicity, it is assumed that kinetics of the monomer-starved styrene semibatch emulsion polymerisation during growth stage can be also approximated by a zero–one system. This assumption can be justified because of the large number of polymer particles formed under monomer-starved conditions which transforms the kinetic of the polymerisation to case I and more important because of the rate of polymerisation during feeding being tightly controlled by the rate of monomer addition. This assumption should be lifted when the molecular weights or particle size distributions of latexes are modelled.
- Monomer transfer from the fed-in monomer droplets to the monomer-starved polymer particles is instantaneous so that no monomer droplets are formed in the reaction mixture during feeding.
- A monodispersed population represents polymer particles.
- The monomer solubilisation in micelles and dissolution in the water phase are considered. These are of quite importance for the early minutes of the polymerisations

when the overall monomer concentration in the reacting latex is low.

- Equilibrium is assumed to be maintained during polymerisations among all phases (the monomer concentrations in different phases are at thermodynamic equilibrium).
- Entry into micelles and polymer particles occurs when radicals reach a critical size of z.
- Diffusional mechanism is assumed to be dominant for the entry of the radicals into polymer particles and micelles, indicating that the entry rate constant varies with the size.
- A distinction is made between oligoradicals generated from the decomposition of the initiator in the water phase and those formed from monomeric desorbed radicals.
- Only monomeric radicals can desorb the polymer particles.
- The fate of the exited free radicals is either to re-enter polymer particles or to terminate in the water phase.
- The end of micellar nucleation is marked by the time that all emulsifier micelles are depleted.
- The monomer concentration in polymer particles varies with their size.
- In view of the high concentrations of emulsifier, particle coagulation is assumed to be negligible.
- The rate of initiator decomposition does not vary with monomer concentration in the water phase.

2.2.1. Material balances

The material balance for styrene is

$$\frac{\mathrm{d}[M]}{\mathrm{d}t} = -R_\mathrm{p} + \frac{R_\mathrm{a}\rho_\mathrm{m}}{M_\mathrm{mon}} \tag{29}$$

where $[M]$ is the total number of moles of monomer in the reactor per litre of water phase, M_mon is the molecular weight of the styrene monomer, and R_p is

$$R_\mathrm{p} = \frac{\mathrm{d}[P]}{\mathrm{d}t} = \frac{k_\mathrm{p}[M]_\mathrm{p}N_\mathrm{p}\bar{n}}{N_\mathrm{A}} \tag{30}$$

where $\bar{n}$ is the average number of radicals per particle, $[M]_\mathrm{p}$ is the monomer concentration in polymer particles, $[P]$ is the total number of moles of monomer converted per litre of water phase, and N_A is the Avogadro's number. For simplicity, all balance equations are written in terms of a litre of water phase. The initial value for $[M]$ at $t = 0$ is $[M]_0$. The material balance for the initiator is as follows:

$$\frac{\mathrm{d}[I]}{\mathrm{d}t} = -k_\mathrm{d}[I] \tag{31}$$

For the styrene monomer, the rate of polymerisation in the water phase is negligible, and thus was ignored. The instantaneous conversion at time t is defined as the weight ratio of the polymer formed in the reactor to the total monomer fed into the reactor by time t:

$$x_i = \frac{(R_\mathrm{a}t\rho_m + [M]_0M_\mathrm{mon}) - [M]M_\mathrm{mon}}{(R_\mathrm{a}t\rho_\mathrm{m} + [M]_0M_\mathrm{mon})} \tag{32}$$

The overall conversion is defined as the weight ratio of the polymer in the reactor to the total monomer in the recipe

$$x_o = \frac{(R_\mathrm{a}t\rho_\mathrm{m} + [M]_0M_\mathrm{mon})x_i}{[M]_\mathrm{t}M_\mathrm{mon}} \tag{33}$$

where $[M]_\mathrm{t}$ is the total number of moles of monomer in the recipe per litre of the water phase.

2.2.2. Rate of particle formation

The rate of particle formation is the sum of particle formation by homogeneous and micellar nucleations. For the styrene emulsion polymerisation at the condition of this study, the contribution of homogeneous nucleation to the overall particle formation is not appreciable. However, it was included in the model.

$$\frac{\mathrm{d}N_\mathrm{p}}{\mathrm{d}t} = k_\mathrm{pw}^{j_\mathrm{cr}-1}[IM^\circ_{j_\mathrm{cr}-1}][M]_\mathrm{w} + \rho_{i,\mathrm{micelle}}N_\mathrm{m} \tag{34}$$

where $\rho_{i,\mathrm{micelle}}$ is the total rate coefficient for entry of initiator-derived radicals into a micelle and N_m is the micelle concentration.

2.2.3. Rate coefficients for radical entry

Hansen and Uglestad [12] suggested that the absorption efficiency of radicals is a function of their partition coefficient between particles and water. It is assumed that the growth of the aqueous phase free radicals to a particular degree of polymerisation, z, is the rate-determining step for free radicals captured by either latex particles or monomer-swollen micelles [14,15]. The total rate coefficient for radical entry into a micelle is given by

$$\rho_{i,\mathrm{micelle}} = \sum_{i=z}^{j_\mathrm{cr}-1} k^i_\mathrm{am}[IM^\circ_i] \tag{35}$$

where $[IM^\circ_i]$ is the concentration of initiator-derived radicals with the chain length i, k^i_am is the rate coefficient for radical entry of length i into a micelle of radius r_m given by:

$$k^i_\mathrm{am} = 4\pi D_i r_\mathrm{m} N_\mathrm{A} \tag{36}$$

D_i is the diffusion coefficient of radicals with chain length i in the water phase which is simply corrected with the diffusion coefficient of monomer in the water phase, D_w, through $D_i = D_\mathrm{w}/i$.

2.2.4. Polymer particles population balances

The rate equations for the polymer particles with no radical (N_0), one monomeric radical (N^m_1), and one polymeric radical (N^p_1) are as follows

$$\frac{\mathrm{d}N_0}{\mathrm{d}t} = \rho(N^\mathrm{p}_1 + N^\mathrm{m}_1 - N_0) + k_\mathrm{dM}N^\mathrm{m}_1 \tag{37}$$

$$\frac{\mathrm{d}N^\mathrm{m}_1}{\mathrm{d}t} = \rho_\mathrm{reentry}N_0 - \rho N^\mathrm{m}_1 - k_\mathrm{dM}N^\mathrm{m}_1 + k_\mathrm{tr}[M]_\mathrm{p}N^\mathrm{p}_1 - k^1_\mathrm{p}[M]_\mathrm{p}N^\mathrm{m}_1 \tag{38}$$

$$\frac{dN_1^p}{dt} = \rho_{i,particle}N_0 - \rho N_1^p - k_{tr}[M]_p N_1^p + k_p^1[M]_p N_1^m + \frac{dN_p}{dt} \quad (39)$$

where k_p^1 is the propagation rate coefficient of a monomeric radical formed by transfer. $\rho_{i,particle}$, the total rate coefficient for entry of initiator-derived radicals into a particle, is

$$\rho_{i,particle} = \sum_{i=z}^{j_{cr}-1} k_{ap}^i[IM_i^\circ] \quad (40)$$

and ρ, the total rate coefficient for radical entry into a particle, is the sum of two components as follows:

$$\rho = \rho_{i,particle} + \rho_{reentry} \quad (41)$$

k_{ap}^i is the rate coefficient for radical entry of length i into a polymer particle with a swollen radius r_p, which is given by

$$k_{ap}^i = 4\pi D_i r_p N_A \quad (42)$$

For a full description of physical and chemical phenomena involved, readers are referred to the book of Gilbert [15].

For a zero–one system, the average number of radicals per particle is simply defined as:

$$\bar{n} = \frac{N_1^p + N_1^m}{N_p} \quad (43)$$

2.2.5. Rate coefficients for radical desorption and re-entry of the desorbed radicals

k_{dM}, the first-order rate coefficient for desorption of a radical from a polymer particle, is given by Refs. [13,20–22]:

$$k_{dM} = \frac{3D_pD_w}{(aD_p + D_w)r_p^2} \quad (44)$$

where D_p and D_w are the diffusion coefficients of the desorbing species, monomeric radicals, in the polymer phase and in the water phase, respectively, and a is the partition coefficient of monomeric radicals (or monomer) between the polymer phase and the aqueous phase ($[M]_p/[M]_w$). As polymerisation proceeds in the particles under monomer-starved conditions, the particles become more glassy and the monomer diffusion becomes very slow. The provision for variation of D_p with conversion is presented in Section 2.2.7. The total rate coefficient for re-entry of the desorbed radicals into a polymer particle is

$$\rho_{reentry} = k_{eE}[E^\circ] \quad (45)$$

k_{eE} is the rate coefficient for re-entry of a desorbed radical to a polymer particle and is given by

$$k_{eE} = 4\pi D_i r_p N_A \quad (46)$$

2.2.6. Radical balances in the aqueous phase

The oligomeric radicals (IM_i) formed by the initiator decomposition in the water phase can have different fates: entry into micelles, entry into particles, propagation, and termination in the water phase. Using the steady-state approximation to the rate equations for oligomers up to $i = j_{cr} - 1$, we have

$$[IM_1^\circ] = \frac{2k_d[I]}{k_{pw}^1[M]_w + k_{tp}[R^\circ]} \quad (47)$$

$$[IM_i^\circ] = \frac{k_{pw}^{i-1}[IM_i^\circ][M]_w}{k_{pw}^i[M]_w + k_{tw}[R^\circ]} \quad i = 2,\ldots,z-1 \quad (48)$$

$$[IM_i^\circ] = \frac{k_{pw}^{i-1}[IM_{i-1}^\circ][M]_w}{k_{pw}^i[M]_w + k_{tw}[R^\circ] + k_{ap}^i N_p + k_{am}^i N_m} \quad (49)$$

$i = z,\ldots,j_{cr-1}$

The total aqueous phase radical concentration is

$$[R^\circ] = \sum_{i=1}^{j_{cr-1}} [IM_i^\circ] \quad (50)$$

The rate equation for exited radicals E° is

$$\frac{d[E^\circ]}{dt} = k_{dM}N_1^m - \rho_{reentry}N_p - k_{tw}[E^\circ][R^\circ] \quad (51)$$

The rate coefficient of radical propagation in the water phase was assumed to vary with degree of polymerization [15].

2.2.7. Diffusion limitations in polymer particles

Zero–one system usually refers to the systems in which instantaneous radical termination occurs as soon as the second radical enters a particle containing an active radical. One of the important features of monomer-starved semi-batch emulsion polymerisation systems is that they are operated at a high polymer weight ratio in the particles at which the termination reaction becomes diffusion controlled and thus, the rate of termination is significantly reduced. This will result in an accumulation of radicals in polymer particles. However, the termination reaction does not play an important role for a system in which the rate of radical entry is much lower than the rate of radical desorption ($\bar{n} \ll 0.50$), and also the rate of polymerisation is controlled by the rate of monomer addition. Therefore, it was ignored in the context of this study.

In the high-conversion regime the rate of propagation often become diffusion-controlled. As a result, the value of k_p will reduce with conversion. The reduction in k_p at high conversions is predicted by the following empirical equation [23–25]

$$k_p = k_{p0} \qquad \text{when } V_f \geq V_{f,cr} \quad (52)$$

$$k_p = k_{p0} \exp\left[-A\left(\frac{1}{V_f} - \frac{1}{V_{f,cr}} \right) \right] \qquad \text{when } V_f < V_{f,cr} \quad (53)$$

where k_{p0} is the intrinsic propagation rate constant, V_f is the fractional free volume of the polymer particles, $V_{f,cr}$ is the V_f at the onset of glass effect, and A is a constant. The fraction free volume of the polymer phase can be calculated by the following equation

$$V_f = V_{fm}\varphi_m + V_{fp}\varphi_p \quad (54)$$

where V_{fm} and V_{fp} are the fractional free volumes of monomer and polymer, respectively. $\varphi_p (= 1 - \varphi_m)$ can be easily correlated with w_p. V_{fm} and V_{fp} are calculated as follows:

$$V_{fm} = 0.025 + \alpha_m (T - T_{gm}) \quad (55)$$

$$V_{fp} = 0.025 + \alpha_p (T - T_{gp}) \quad (56)$$

where α_m and α_p are the thermal expansion coefficients of monomer and polymer, respectively. T_{gm} and T_{gp} are the glass transition temperatures of monomer and polymer, respectively.

The decrease in the propagation rate constant at high conversions is in fact the result of a reduction in the diffusion coefficient of monomer molecules in the polymer phase. Therefore, the variation of D_p with polymer phase ratio can be easily obtained by:

$$D_p = D_{p0} \frac{k_p}{k_{p0}} \quad (57)$$

where D_{p0} is the diffusion coefficient of desorbing monomeric radicals before the onset of glass effect.

2.2.8. Emulsifier partitioning

For a monomer-starved semibatch emulsion polymerisation, surfactant partitions among the three sites available: polymer particles, micelles, and water phase. Assuming that surfactant concentration stays at the critical micellar concentration (CMC) value and the polymer particles are fully covered by emulsifier molecules, the concentration of micelles during nucleation is found with the following equation:

$$N_m = ([S]N_A - (3V_p)^{2/3}(4\pi N_p)^{1/3}/a_s - [S_{CMC}]N_A)/n_{agg} \quad (58)$$

where n_{agg} is the aggregation number of micelles which is subject to variation in the course of reactions, as is described in Section 2.2.9. In evaluating N_m, the average size of particles has been used. An allowance could be made for the particle size distribution. However, this does not introduce an appreciable error to the calculations.

2.2.9. Monomer partitioning

In our previous publication, we described a routine for estimation of monomer partitioning among different phases from the conversion-time data [4]. Here, we use a more vigorous version of the routine with conjunction with the model. The following equations give the distribution of monomer among polymer particles, the water phase, and micelles. The dissolution of water in micelles and polymer particles is ignored.

$$[M]_w = [M]_{w,sat} \left(\frac{[M]_p}{[M]_{p,sat}} \right)^{0.60} \quad (59)$$

$$[M]_m = K_{eq}[M]_w N_m / N_A \quad (60)$$

$$[M]_p = \frac{[M] - [M]_w - [M]_m}{V_p} \quad (61)$$

Eq. (59) is an empirical correlation which correlates the monomer concentration in the polymer phase ($[M]_p$) with that in the aqueous phase, $[M]_w$ [14,26]. $[M]_{p,sat}$ and $[M]_{w,sat}$ are the monomer concentrations in the polymer phase and in the water phase under saturation conditions, respectively. The dependence of saturation monomer concentration in particles on the particle size can be expressed by Morton's equation, but it is simpler to use a semiempirical form as follows [27]

$$[M]_{p,sat}(r_p) = [M]^{\infty}_{p,sat} \tanh\left(\frac{r_p}{r_F} \right) \quad (62)$$

where $[M]^{\infty}_{p,sat}$ is the large-diameter limiting value of $[M]_{p,sat}$, and r_F is a fitting parameter. The value for r_p at any time is obtained from the following equation

$$r_p = \left(\frac{3V_p}{4\pi N_p} \right)^{1/3} \quad (63)$$

where V_p is the volume of the polymer phase per litre of water phase. Eq. (60) is a variation of the correlation originally proposed by Almgren [28] in which $[M]_m$ is the number of moles of monomer solubilised in micelles per litre of water phase. As a general rule, the CMC value and the aggregation number of an ionic surfactant are influenced by the presence of the solutes, such as electrolytes, and water insoluble compounds in the water phase. The number of molecules of styrene solubilised in a micelle, X_M, can be easily obtained from Eq. (60) ($X_M = [M]_m N_A / N_m$). As X_M decreases with $[M]_w$ in the course of polymerisation, the micelles shrink and as a result, some emulsifier molecules are released into the water phase and form new micelles. The size variation of micelles is conformed to a constant surface coverage ratio of emulsifier molecules. An increase in the aggregation number of micelles with $[M]_w$ is given by Ref. [29]

$$\Delta n_{agg} = 2K_{eq}[M]_w \frac{V_M}{V_S} \quad (64)$$

where V_S and V_M are the hydrophobic volumes of the surfactant tail and monomer, respectively. The overall aggregation number of a monomer-swollen micelle is

$$n_{agg} = n_{agg0} + \Delta n_{agg} \quad (65)$$

where n_{agg0} is the aggregation number in the non-swollen

Table 1
The parameters used for simulation of styrene emulsion polymerisation at 70 °C

Parameter	Value	Reference
k_{pw}^1 (l/mol s)	1300	[15]
k_{pw}^2 (l/mol s)	840	[15]
k_{pw} (l/mol s)	480	[15]
k_{tw} (l/mol s)	3×10^9	[15]
D_w (cm^2/s)	1.5×10^{-5}	[15]
D_{p0} (cm^2/s)	1.5×10^{-5}	[15]
$[M]_{p,sat}^{\infty}$ (mol/l)	5.8	[15]
$[M]_{w,sat}$ (mol/l)	5.6×10^{-3}	[15]
j_{cr}	5	[15]
k_{tr} (l/mol s)	9.3×10^{-3}	[15]
k_{p0} (l/mol s)	480	[15]
k_p^1 (l/mol s)	$4\ k_p$	[15]
ρ_m (g/cm^3)	0.878	[15]
ρ_p (g/cm^3)	1.044	[15]
r_F (nm)	8	[27]
$V_{f,cr}$	0.033	[25]
α_m (1/°C)	0.001	[25]
α_p (1/°C)	4.8×10^{-4}	[25]
T_{gm} (°C)	−88.2	[25]
T_{gp} (°C)	93.5	[25]
A	1	[29]
α_s (Å^2)	43	[15]
S_{CMC} (mol/l)	3.9×10^{-3}	[15]
n_{agg0}	80	[29]
V_S (nm^3)	385	[29]
V_M (nm^3)	197	[29]
K_{eq} (l/mol)	1.68×10^4	[29]
k_d (1/s)	2.2×10^{-5}	[15]

state. From n_{agg} and X_M it is now possible to estimate the variation of the volume of a micelle, and thus its radius r_m, in the course of feeding. The volume of a micelle in the course of polymerisation is the sum of contributions from the hydrophobic volumes of the surfactant tail and monomer from which the radius of micelles can be easily obtained as:

$$r_m = (3(n_{agg}V_S + X_M V_M)/4\pi)^{1/3} \tag{66}$$

V_p is given by:

$$V_p = R_a t + \left([M]_0 - [M]_w - [M]_m - [P]\left(1 - \frac{\rho_m}{\rho_p}\right)\right)\frac{M_{mon}}{\rho_m} \tag{67}$$

The corresponding value for polymer weight ratio in the polymer particles, w_p, for any $[M]_p$ can be obtained from the following equation

$$w_p = \frac{[M]_p M_{mon} - \rho_m}{[M]_p M_{mon}\left(1 - \frac{\rho_m}{\rho_p}\right) - \rho_m} \tag{68}$$

2.2.10. Model implementation

Model II was integrated by using a fourth order Runge–Kutta algorithm with a variable step size. Eqs. (29)–(60) and (62)–(68) are numerically solved, while z was treated as an adjustable parameter. The rate constants and the parameters required for the mathematical modelling are all obtained from the literature and are listed in Table 1. The determination of $[M]_p$ involves a trial-and-error procedure. For each step a value for $[M]_p$ is assumed, and the above-mentioned equations are solved, The values for $[M]$, $[M]_w$, $[M]_m$, and V_p, obtained from Eqs. (29), (59), (60) and (67), respectively, are used to calculate $[M]_p$ through Eq. (61). The calculated value is compared with the guessed value. A new value for $[M]_p$ is guessed if there is not agreement. This cycle continues until the guessed value and the calculated value are within a tolerance of $\pm 10^{-2}$%. It should be noted that although model II is presented for monomer-starved conditions, it can be used, with a minor modification, to fit monomer-flooded conditions. In fact, the inclusive version of the model should be always used in prior to any analysis, to assure that monomer-starved conditions are always attained in the system under study.

The models are used to analyse the kinetic data of the semibatch emulsion polymerisation of styrene reported in our previous publication [4]. The semibatch emulsion polymerisation reactions (70 °C) were started by monomer being fed at a low rate to the reaction vessel containing de-ionised water, an emulsifier (sodium lauryl sulphate, SLS), and an initiator (potassium persulphate, KPS). A very small amount of monomer (1.78 mmol/l for most runs) was also placed in the initial charge. Three sets of experiments with [SLS], [KPS] and R_a as variables were carried out. They were named sets 1–3, respectively. The formulations for sets 1–3 are given in the caption of Fig. 1.

3. Results and discussion

3.1. Number of polymer particles

The model predictions for the exponents, together with the experimental values, are listed in Table 2. Fig. 1 compares predicted, based on model I, and observed particle number as a function of variations in [SLS] − S_{CMC}, [KPS], and R_a, respectively. The value of $f = 0.13$ was found to give the best fits to the number of particles for all sets of the experiments, while the slopes were independent of the f value.

Fig. 2 presents the prediction of model II for N_p with [SLS] − S_{CMC}, [KPS], and R_a, respectively. All the experimental exponents fall within the range of predictions of the SE theory for conventional batch process and its extended version for the semibatch processes under monomer-starved conditions. Generally, with a decreasing z value, the slopes of the N_p curves increase and eventually approach those predicted by model I. Similar to the results reported by Maxwell et al. no single value of z can provide a perfect fit to all the data [14]. For N_p, a z value of 2 always gives the best fit to the data. For the exponents, the z value of

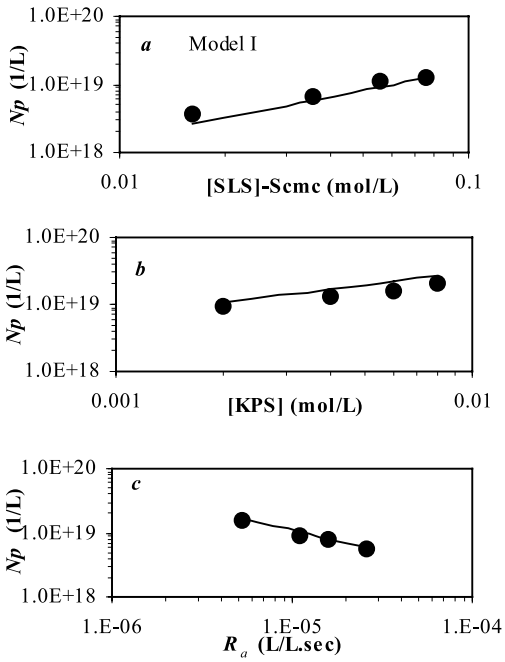

Fig. 1. Comparison between model-I predictions (–) and the experimental data (●) for N_p versus (a) [SLS] (set 1: [KPS] = 2 mmol/l, $R_a = 2.6 \times 10^{-5}$ l/l s), (b) [KPS] (set 2: [SLS] = 40 mmol/l, $R_a = 1.05 \times 10^{-5}$ l/l s), (c) R_a (set 3: [SLS] = 40 mmol/l, [KPS] = 2 mmol/l).

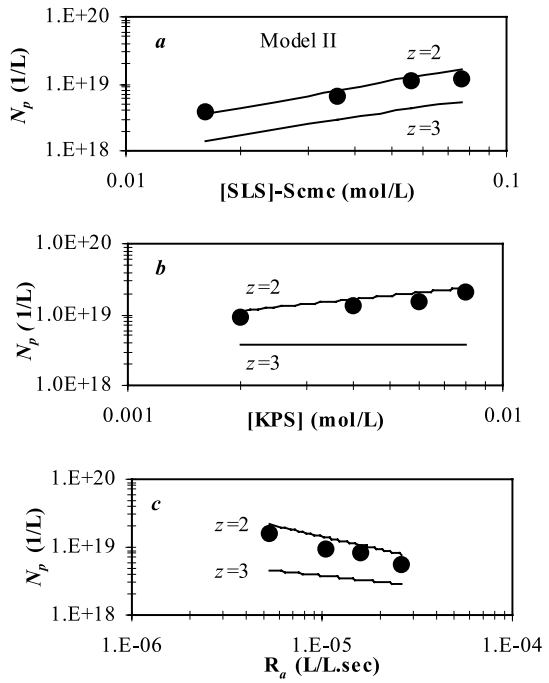

Fig. 2. Comparison between the model-II predictions (–) and the experimental data (●) for N_p versus (a) [SLS], (b) [KPS], and (c) R_a (see caption of Fig. 1 for the conditions).

2 also gives a better agreement for N_p – [KPS] and N_p – R_a curves. But the z value of 3 gives a better approximation for the exponent of N_p – [SLS] curve (Table 2). As a general statement, the number of particles and the slopes of the theoretically calculated lines using $z = 2$ are closer to those found experimentally. Similarly, Lopez de Arbina et al. [16] found that a z value of 2 gives a better fit to the styrene emulsion polymerisation during growth stage. As the z value reduced from 3 to 2, the predictions of model II approached those of model I (Table 2).

3.2. Rate of polymerisation

Fig. 3a and b compares the model II predictions and the conversion-time data for different SLS concentrations and z values. The z value of 2 overestimates the conversions in the first hour of the feedings, but can satisfactorily predict the conversions in the later stage of the polymerisations.

Table 2
The comparison of experimental and theoretical N_p exponents

Sets	Theory			Experimental
	Model I	Model II		
		$z = 2$	$z = 3$	
Set 1: N_p versus [SLS] – S_{CMC}	1.00	1.00	0.87	0.80
Set 2: N_p versus [KPS]	0.67	0.54	0.04	0.55
Set 3: N_p versus R_a	−0.67	−0.63	−0.32	−0.65

Whereas the z value of 3 predicts properly the early conversions, but underestimates the conversion at a later stage of feeding.

Fig. 4 shows the conversion-time data for different KPS concentrations and z values. Both z values overestimate the initial rate of polymerisations, but give proper estimations at a later stage. At a fixed z value, x_i was not influenced by [KPS]. This set of experiments was conducted with a lower R_a than the one used for set 1 (for the comparisons see caption of Fig. 1). The difference between the experimental data and the model predictions becomes more evident if a lower R_a is used. It is also observed from Figs. 3 and 4 that in accordance with the experimental conversion-time data during the growth stage, the model predictions are not significantly affected by alteration in the formulation variables such as [SLS] and [KPS].

Newly formed particles mostly undergo radical exit, before the second radical can enter them. Model II predicts that for the conditions of this study $\bar{n}$ is less than 0.3 and 0.1 during growth stage with z values of 2 and 3, respectively. This is in accord with the experimental value reported for $\bar{n}$ which is lower than 0.1 [4]. Therefore, the application of zero–one assumption to the growth stage can be justified in the context of this study.

Although the models can successfully predict some important aspects of the particle formation under monomer-starved conditions, one question remains unanswered; that is the low rate of polymerisation in the early minutes, and in some cases in the early hours, of the feedings. A possible reason for this could be the limitations in monomer diffusion

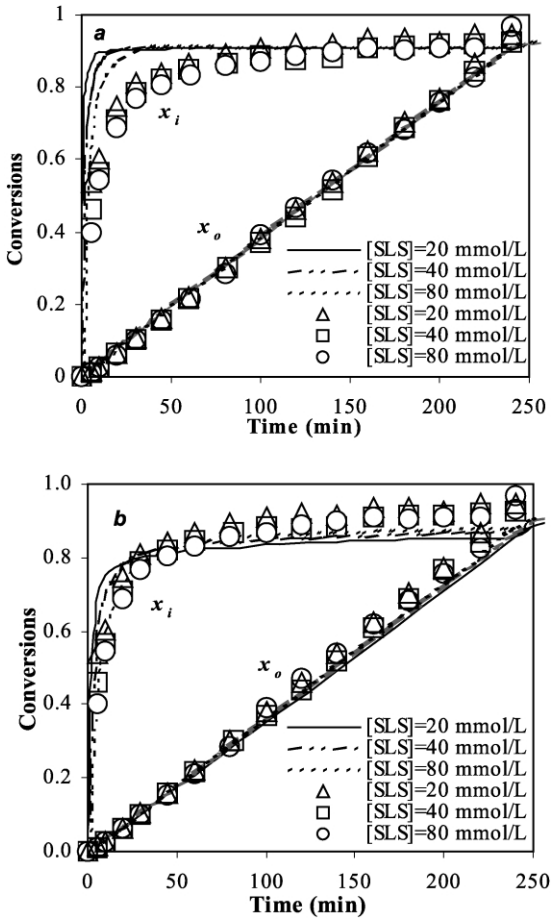

Fig. 3. Model predictions (–) versus experimental conversions (symbols) for different [SLS] and z values of (*a*) $z = 2$, and (b) $z = 3$ (set 1).

[30]. A very low monomer uptake by the small primary polymer particles, lower than that predicted by Eq. (62), could also explain the reduced rate of polymerisation. Despite all these speculations, the true reason for the low rate of reaction in the initial stage of the polymerisations is not clear at this stage of research and further clarifications are required.

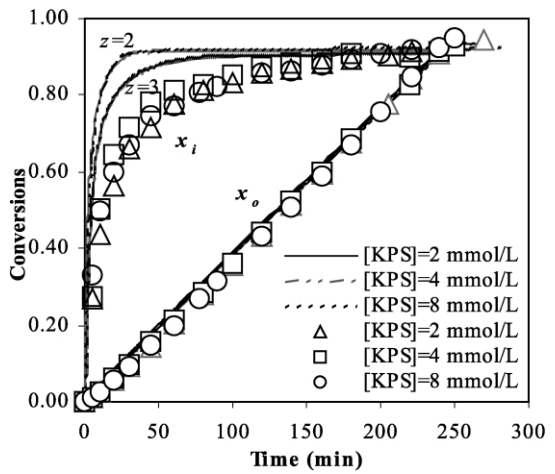

Fig. 4. Model predictions (–) versus experimental conversions (symbols) for different [KPS] and z values of 2 and 3 (set 2).

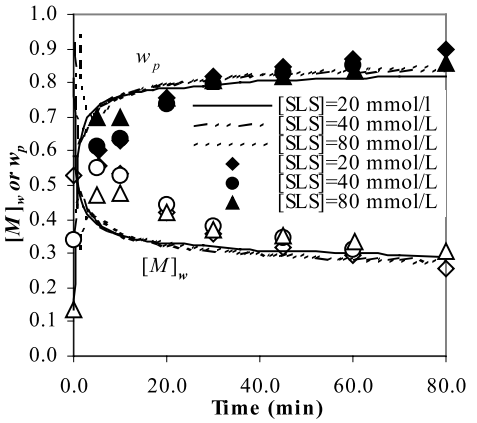

Fig. 5. Predicted (–) and experimental w_p (closed symbols) and $[M]_w$ (open symbols) for different [SLS] and $z = 3$. $[M]_w$ is given in terms of g/l (set 1).

3.3. Dynamic of the polymerisations

Fig. 5 compares the model predictions and the experimental data for w_p and $[M]_w$ at different [SLS]. The results from the runs with $z = 3$ were selected for the analysis because they can give a better fit to the early conversion-time data. $[M]_w$ in the initial stage of the polymerisations is low because the polymerisations started with a very low monomer concentration. As the monomer addition started, the monomer accumulates in the system because of a low initial rate of polymerisation. As a result $[M]_w$ increases to a maximum and then decreases slowly in the course of monomer addition. In contrast, w_p starts decreasing from a value as high as 0.95, decreases to a minimum value as more monomer accumulates in the reacting mixture and then starts increasing. The magnitude of variations of w_p and $[M]_w$ with time depends on [SLS], as shown in Fig. 5.

Fig. 6 indicates that in accordance with the variations in $[M]_w$, micelles dilate in the early minutes but shrink afterwards. Accordingly, n_{agg} and X_M start from the initial values, and after going through a maximum, decrease with time. For the lower [SLS], the maximum appeared in the first few moments of polymerisation and afterwards both n_{agg} and X_M decreased with time. As [SLS] increased, the maximum was reduced in magnitude and appeared at a later time.

Fig. 7 compares the number of moles of monomer in the polymer phase ($[M_{pw}] = [M]_p V_p$), micelle phase, and water phase per litre of water phase for two SLS concentrations. The overall number of moles of monomer per litre of water phase ($[M]$) is also shown. As expected, $[M]_m$ increases with [SLS]. As micelles disappear with time, $[M]_m$ is reduced and correspondingly $[M]_{pw}$ increases. At [SLS] = 20 mmol/l, most of the monomer accumulates in the polymer particles ($[M]_{pw} > [M]_m$) from early in the reaction. At [SLS] = 80 mmol/l, most of the monomer resides in the micelles during the first 10 min of the polymerisation ($[M]_m > [M]_{pw}$), but gradually with the

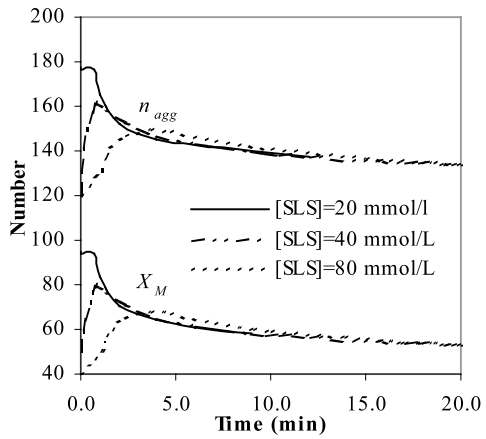

Fig. 6. Model predictions for time evolution of X_M and n_{agg} for different [SLS] and $z = 3$ (set 1).

depletion of emulsifier micelles $[M]_m$ is reduced to a lower value than $[M]_{pw}$.

3.4. Effect of $[M]_w$ on nucleation

Semibatch emulsion polymerisations can often be characterised by a continuous variation in $[M]_w$, as revealed in Figs. 5 and 7. Any variation in formulation variables, will

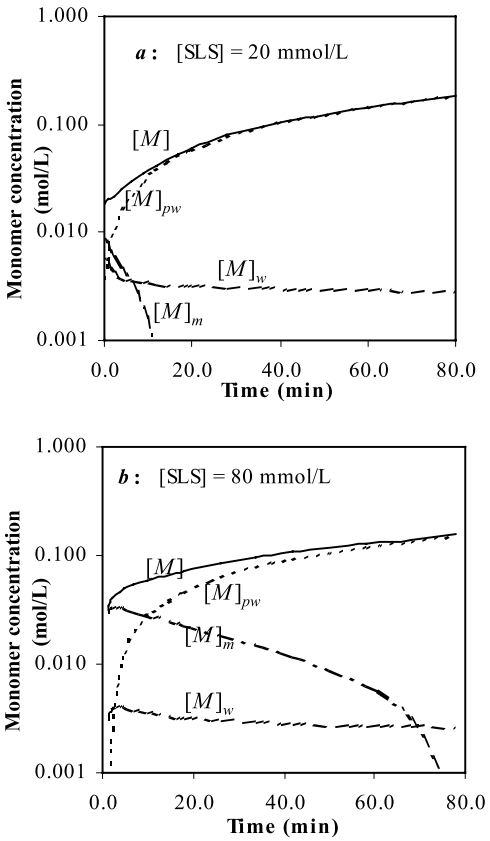

Fig. 7. Model predictions for the time evolution of number of moles of unreacted monomer in the reactor ($[M]$), polymer phase ($[M]_{pw}$), micelles ($[M]_m$), and water phase ($[M]_w$) per litre of water phase for two SLS concentrations of (a) 20 and (b) 80 mmol/l and $z = 3$ (set 1).

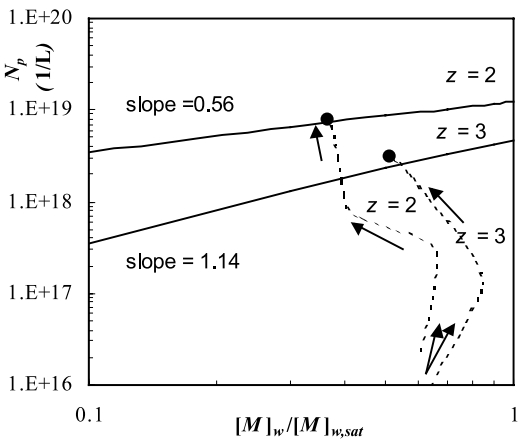

Fig. 8. Variation in N_p with $[M]_w/[M]_{w,sat}$ for an ideal polymerisation system with [SLS] = 40 mmol/l, [KPS] = 2 mmol/l, and $R_a = 2.6 \times 10^{-5}$ l/l s. The dashed lines show the actual evolution of N_p for the corresponding polymerisation runs with $z = 2$ and 3, with the final N_p shown by (●).

inevitably affect the time evolution of $[M]_w$ in the course of nucleation, which in turn can affect nucleation. This is quite different from conventional nucleation during which $[M]_w$ is always constant at the saturation value. Perhaps the most important feature of the entry model adopted in this research is that it can reflect the effects of variations in $[M]_w$ on the whole nucleation process.

To elucidate the effect of $[M]_w$ on N_p, we consider an ideal monomer-starved semibatch emulsion polymerisation system for which nucleation could occur at a constant $[M]_w$. Fig. 8 shows the variation in the predicted N_p, for the polymerisation specified in the caption of the figure, with $[M]_w/[M]_{w,sat}$. N_p shows an appreciable increase with $[M]_w/[M]_{w,sat}$. The probability of reaching the chain length of z for a growing radical, depends, amongst other factors, on $[M]_w$. With a higher $[M]_w$, a faster propagation rate for radicals would allow for more radical entry into micelles (and particles) compared with termination in the water phase. With $z = 2$, the rate of radical entry into monomer swollen micelles and particles is usually less sensitive to variation in $[M]_w$ than that with $z = 3$. The slopes of N_p-$[M]_w/[M]_{w,sat}$ curves were found to be 0.56 and 1.14 with z values of 2 and 3, respectively. These slopes are not constant and can vary with the polymerisation conditions. The evolution of predicted N_p with $[M]_w/[M]_{w,sat}$ for the same formulation, but under actual conditions in which $[M]_w$ is continuously changing during nucleation, is also shown on the same figure. The polymerisation run started with $[M]_w/[M]_{w,sat} = 0.6$, but the ratio varied in the course of polymerisation. With $z = 2$, most of the nucleation occurred at $[M]_w/[M]_{w,sat} = 0.40$, and the N_p predicted is almost corresponding to this ratio. With $z = 3$, most of the particles were formed within $[M]_w/[M]_{w,sat} = 0.50–0.70$ and eventually an average N_p corresponding to this range was obtained.

It is quite important to realise the most important

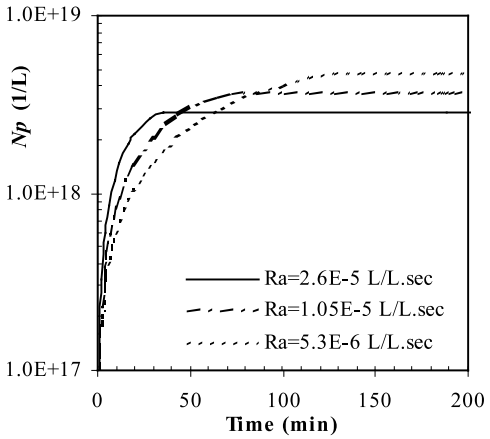

Fig. 9. Model predictions for the time evolution of N_p for different R_a and $z = 3$ (set 1).

parameters which can affect $[M]_w$. Here, we briefly discuss some of these parameters. Any increase in R_a, for example, will simultaneously increase $[M]_w$ and μ. The former increases N_p by enhancing the rate of radical entry into micelles, leading to a larger initial rate of particle formation (dN_p/dt), as shown in Fig. 9. The latter reduces N_p by increasing the rate of depletion of emulsifier micelles, leading to a shorter nucleation time and a lower final N_p. As a result of these opposite trends, the $N_p - R_a$ exponent predicted by model II, is often smaller than that predicted by model I (Table 2).

The variations of $[M]_w$ with [SLS], as shown in Figs. 5 and 7, have some interesting consequences. In the early minutes of feeding, the emulsifier micelles behave as monomer reservoirs. As the number of emulsifier micelles increases with [SLS], a larger proportion of monomer is solubilised in the micelles and less accumulates in the water phase and in the newly formed particles (less $[M]_p$ and $[M]_w$). Fig. 10 shows the predictions of model II for the time evolution of N_p for different SLS concentrations. The initial rate of particle formation shows an increase with decreasing [SLS] because of a higher $[M]_w$ (Figs. 5 and 7). However,

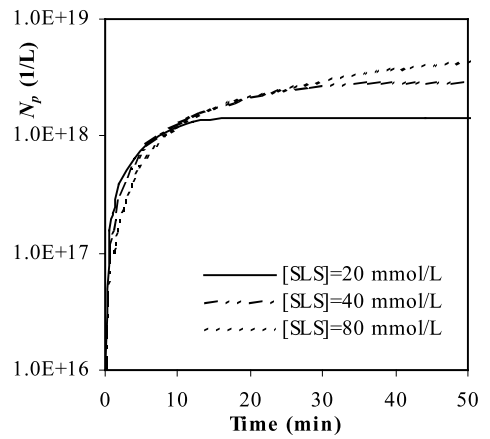

Fig. 10. Model predictions for the time evolution of N_p for different [SLS] and $z = 3$ (set 1).

particle formation lasts for a longer period of time for the higher [SLS], leading to a larger N_p. Less distinction can be found for the time evolutions of N_p in terms of [SLS] with $z = 2$. Unfortunately, the time evolution of N_p during nucleation was not monitored. The conversion-time data, however, can be used to support this finding. Because of increase in $[M]_p$ and $[M]_w$, a higher initial rate of polymerisation is expected for the lower [SLS], a trend which is quite obvious in the experimental data depicted in Fig. 3a and b. Furthermore, these figures show that the model can satisfactorily predict the increase in the initial rate of polymerisation with decreasing [SLS]. Generally, as a result of variation in $[M]_w$ during nucleation, the $N_p - [SLS]$ exponent predicted by model II (with $z = 3$) is smaller than that predicted by model I.

Perhaps one of the most distinctive features of entry model of Maxwell et al. is its capability to explain the deviation of experimental $N_p - [I]$ exponent from the prediction of SE theory for conventional batch emulsion polymerisation. As z increases, more radical termination in the water phase occurs and the exponent decreases. Radical termination in the water phase is enhanced with decreasing $[M]_w$ under monomer-starved conditions. This can even lead to a further reduction in the predicted $N_p - [KPS]$ exponents.

3.5. Sensitivity analysis

It is important to assess the sensitivity of model-II predictions to some of the crucial assumptions made in its development. The simulation results obtained for $N_p - [SLS]$ are selected and shown as the reference line in Fig. 11. The results of sensitivity analysis are compared with the reference line.

(1) *Monomer solubilisation in micelles*. Now that the effects of $[M]_m$ on the evolution of N_p and R_p were described and shown to be important, we further study the effect of $[M]_m$ on the final N_p. The simulation results for $[M]_m = 0$ are shown in Fig. 11. In comparison with the reference line, N_p showed an increase with $z = 3$, but remained constant with $z = 2$ (the latter falls on the reference line). Correspondingly, $N_p - [SLS]$ exponent for $z = 3$ changed from 0.87 to 0.93, but remained unchanged for $z = 2$. The underestimation of N_p is the result of increase in the rate of particle growth because of accumulation of monomer in the particles, which could be otherwise solubilised in the micelles (note that this effect counterbalances the effect of concomitant increase in N_p because of a higher $[M]_w$). We previously stated that a higher rate of polymerisation for the lower [SLS] could be only justified on the ground of monomer solubilisation in micelles. Neglecting the amount of monomer solubilised in the micelles will lead to the prediction of high conversions in the early minutes of polymerisation. An unrealistic assumption that could result in a better fit to the conversion-time experimental data. The analysis shows

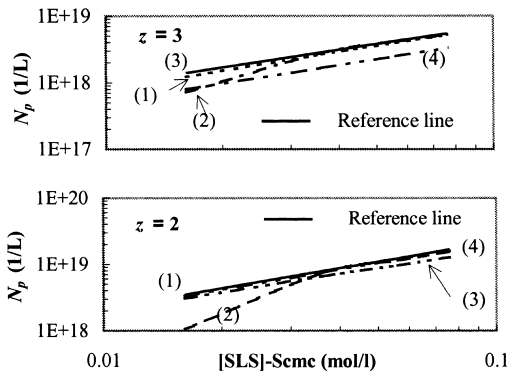

Fig. 11. Variation in N_p with [SLS] − S_{CMC} (mol/1) with model assumptions for z values of 2 and 3. The reference line (–) corresponds to the model predictions with all assumptions considered. The dotted lines represent the model predictions under the conditions that: (1) $[M]_m = 0$, (2): $[M]_p(r)$ = constant, (3): $k_p(V_f)$ = constant, (4) $k_{dM} = 0$.

that although the inclusion of $[M]_m$ in the overall balance of monomer is quite important for tracking the evolution of particle nucleation and monomer conversion, but it does not appreciably affect final N_p and its exponents.

(2) *Monomer concentration in primary particles*. In model II, we accounted for a low saturation monomer concentration in the primary polymer particles. The thermodynamic equilibrium indicates that $[M]_w$ can be high in the presence of small particles, even under monomer-starved conditions. Simulation runs were carried out, with this assumption relaxed ($[M]_p(r) = [M]^{\infty}_{p,sat}$), for different [SLS]. A smaller N_p was obtained in comparison with the reference experiments with both z values. The deviation in N_p from the reference line appears to become more significant with decreasing [SLS] and z, as shown in Fig. 11. When primary particles are allowed to absorb a higher quantity of monomer, they deplete emulsifier micelles very quickly and exhaust the water phase with monomer. Such effects appear to be more important at a lower [SLS] when the concentration of free emulsifier micelles is limited.

(3) *Diffusion-controlled propagation*. Any limitation to propagation, does not appreciably affect the growth rate of particles so long as particles are under monomer-starved conditions and there are no monomer droplets present, but will retard the decreasing trend of $[M]_p$ and $[M]_w$ with time. This enhances the rate of radical entry into monomer-starved micelles and consequently a larger N_p will form. Here we assume that the radical capture efficiency of micelles does not change with the variation in the structure of micelles as they become more starved with monomer. An assumption, which is totally invalid for aerosol-MA surfactant [31], but seems to be acceptable for the current system in view of lack of data. A series of simulation runs were carried out for different [SLS], neglecting the diffusion-controlled propagation ($k_p(V_f) = k_{p0}$), to assess its theoretical effect on N_p. The results are shown in Fig. 11. Generally with $z = 3$, particle nucleation ceases before a high conversion is reached (the results overlap with the reference line). With $z = 2$, a small reduction in the predicted N_p is observed because nucleation could continue into the region, where diffusion-controlled propagation was dominant. This, of course, concomitantly leads to the overestimation of the rate of polymerisation at higher conversions.

(4) *Radical desorption*. Radical exit from particles stops the propagation reaction in polymer particles, retards the accumulation of polymer in the particles and thus increases $[M]_w$. Simulations runs were carried out assuming that no radical exit occurs ($k_{dM} = 0$). The results are illustrated in Fig. 11. As it was expected, N_p is reduced with $z = 3$, compared with the reference line, but it showed little variation with $z = 2$. Correspondingly, the exponent of N_p − [SLS] rose to 0.90 with $z = 3$, but did not change with $z = 2$.

The results from sensitivity analysis suggest that the simple version of model II, which does not include the above-mentioned assumptions, could still give acceptable estimations of final N_p and its exponents with formulation variables, particularly for $z = 2$. This is mainly due to the fact that under monomer-starved conditions, the rate of growth of particles is mainly independent of the kinetics of polymerisation and is determined by the rate of monomer addition, a feature that was used in the development of model I. However, the predictions of time evolution of monomer conversion and N_p can be best carried out if all the assumptions described previously are taken into consideration.

4. Conclusion

Two different approaches were used to predict the final number of polymer particles versus formulation variables for the semibatch emulsion polymerisation of styrene under monomer-starved conditions: (I) SE based model and (II) a dynamic model. The SE theory was extended to cover particle formation under monomer-starved conditions. The application of traditional theory of SE to analyse the experimental data in this research as a first approximation does not underscore the recent advances in understanding of particle formation in emulsion polymerisation reactions. But, it introduces an explicit way to realise the functional dependence of the number of particles on the formulation variables. The effect of decrease in rate of particle growth, caused by radical desorption from polymer particles and/or termination in the particles, on the number of polymer particles was indirectly taken into account by the assumption that the rate of growth of particles is controlled by the rate of monomer addition. A correlation was derived for the prediction of the number of particles formed under monomer-starved conditions. For model II, the kinetic of the water phase was included. It was assumed that entry occurs if radicals can propagate to a critical degree; z. It was shown that a z value of 2 gives the best fit to the experimental data. However, the values of N_p and also the

exponents were not completely reproduced. For N_p − [SLS] and N_p − [KPS], model II gave a better fit, while for N_p-R_a both models could satisfactorily give a good fit. Model II predictions were in agreement with the experimental data of the time evolution of monomer conversion for a high R_a, but failed to reproduce them during nucleation period for the lower R_a. The simulation results show an increasing rate of particle formation with $[M]_w$. This is backed by the experimental data, which indicates an increase in the initial rate of polymerisation with $[M]_w$. To verify this hypothesis, more experimental work is required to focus on the evolution of N_p in the early minutes of polymerisations. Simulations suggest that variations in the exponents can be observed with polymerisation conditions and with the evolution of $[M]_w$.

The treatments developed here make some significant omissions from the real events that might occur during the polymerisation reactions under monomer-starved conditions. The results of these omissions, however, seem to be more quantitative than qualitative. These omissions are:

(1) Limitation in monomer diffusion from fed-in monomer droplets to emulsifier micelles and growing polymer particles.
(2) The decreased rate of radical entry into micelles, caused by variation in the structure of monomer-starved micelles, with monomer conversion.
(3) The monomer concentration in very small primary polymer particles formed under monomer-starved condition might be significantly different from that predicted by the existing correlations.

We feel, however, that these models are adequate in describing the particle formation under monomer-starved nucleation as a first approximation. The models developed here can be extended to incorporate the above-mentioned effects.

References

[1] Smith WV, Ewarts RH. J Chem Phys 1948;16:592.
[2] Gardon JL. J Polym Sci 1968;6:623.
[3] Krackler JJ, Naidus H. J Polym Sci Part C 1969;27:207.
[4] Sajjadi S. J Polym Sci Polym Chem Ed 2001;39:3940.
[5] Sajjadi S, Brooks BW. Chem Engng Sci 2000;55:4757.
[6] Sajjadi S, Brooks BW. J Appl Polym Sci 1999;74:3094.
[7] Greshberg DB, Longfield JE. 54th Annual Symposium Preprint. AICHE, No 10, 1961.
[8] Omi S, Ueda T, Kubota H. J Chem Engng Jpn 1969;2:193.
[9] Gerrens H, Kuchner K. Br Polym J 1970;2:18.
[10] Degraff A, Poehlein GW. J Polym Sci Part 2 1971;9:1955.
[11] Fitch RM, Tsai CH. In: Fitch RM, editor. Polymer colloids. New York: Plenum Press; 1971. p. 73.
[12] Hansen FK, Ugelstad J. J Polym Sci Polym Chem Ed 1978;16:1953.
[13] Hansen FK, Ugelstad J. In: Piirma I, editor. Emulsion polymerisation. New York: Academic Press; 1982. p. 51–92.
[14] Maxwell IA, Morrison BR, Napper DH, Gilbert RG. Macromolecules 1991;24:1629.
[15] Gilbert RG. Emulsion polymerisation: a mechanistic approach. London: Academic press; 1995.
[16] Lopez de Arbina L, Barandiaran MJ, Gugliotta LM, Asua JM. Polymer 1996;37:5907.
[17] Dube MA, Soares JBP, Penlidis A, Hamielec AE. Ind Engng Chem Res 1997;36:966.
[18] Harada M, Nomura M, Kojima H, Eguchi H, Nagata S. J Appl Polym Sci 1972;16:811.
[19] Coen EM, Gilbert RG, Morrison BR, Leube H, Peach S. Polymer 1998;39:7099.
[20] Nomura M. In: Piirma I, editor. Emulsion polymerization. New York: Academic Press; 1982. p. 191–219.
[21] Ugelstad J, Hansen FK. Rubber Chem Technol 1976;49:536.
[22] Harada M, Nomura M, Eguchi W, Nagata S. J Chem Engng Jpn 1971; 4:54.
[23] Arai K, Saito S. J Chem Engng Jpn 1976;9:302.
[24] Soh S, Sundberg DC. J Polym Sci Polym Chem Ed 1982;20:1345.
[25] Martin FL, Hamielec AE. J Appl Polym Sci 1982;27:489.
[26] Ballard MJ, Napper DH, Gilbert RG. J Polym Sci Polym Chem Ed 1984;22:3225.
[27] Feeney PJ, Napper DH, Gilbert RG. Macromolecules 1987;20:2922.
[28] Almgren MF, Grieser F, Thomas JK. J Am Chem Soc 1979;101:279.
[29] Gianetti E. AICHE J 1993;39:1210.
[30] Brooks BW. Br Polym J 1971;3:269.
[31] Sajjadi S. J Polym Sci Polym Chem Ed 2002;40:1652.